JOURNAL OF VIROLOGY, Apr. 2009, p. 3743–3753 Vol. 83, No. 8
0022-538X/09/$08.00+0 doi:10.1128/JVI.02203-08

Organ-Specific Attenuation of Murine Hepatitis Virus Strain A59 by Replacement of Catalytic Residues in the Putative Viral Cyclic Phosphodiesterase ns2[▽]

Jessica K. Roth-Cross,[1]† Helen Stokes,[2]† Guohui Chang,[2] Ming Ming Chua,[1] Volker Thiel,[3] Susan R. Weiss,[1]*‡ Alexander E. Gorbalenya,[4]‡ and Stuart G. Siddell[2]*‡

Department of Microbiology, University of Pennsylvania School of Medicine, Philadelphia, Pennsylvania 19104[1]; Department of Cellular and Molecular Medicine, School of Medical and Veterinary Sciences, University of Bristol, Bristol, United Kingdom[2]; Research Department, Kantonal Hospital St. Gallen, St. Gallen, Switzerland[3]; and Department of Medical Microbiology, Leiden University Medical Center, Leiden, The Netherlands[4]

Received 17 October 2008/Accepted 20 January 2009

The *Murine hepatitis virus* (MHV) strain A59 ns2 protein is a 30-kDa nonstructural protein that is expressed from a subgenomic mRNA in the cytoplasm of virus-infected cells. Its homologs are also encoded in other closely related group 2a coronaviruses and more distantly related toroviruses. Together, these proteins comprise a subset of a large superfamily of 2H phosphoesterase proteins that are distinguished by a pair of conserved His-x-Thr/Ser motifs encompassing catalytically important residues. We have used a vaccinia virus-based reverse genetic system to produce recombinant viruses encoding ns2 proteins with single-amino-acid substitutions in, or adjacent to, these conserved motifs, namely, inf-ns2 H46A, inf-ns2 S48A, inf-ns2-S120A, and inf-ns2-H126R. All of the mutant viruses replicate in mouse 17 clone 1 fibroblast cells and mouse embryonic cells to the same extent as the parental wild-type recombinant virus, inf-MHV-A59. However, compared to inf-MHV-A59, the inf-ns2 H46A and inf-ns2-H126R mutants are highly attenuated for replication in mouse liver following intrahepatic inoculation. Interestingly, none of the mutant viruses were attenuated for replication in mouse brain following intracranial inoculation. These results show that the ns2 protein of MHV-A59 has an important role in virus pathogenicity and that a substitution of the histidine residues of the MHV-A59 ns2 His-x-Thr/Ser motifs is critical for virus virulence in the liver but not in the brain. This novel phenotype suggests a strategy to investigate the function of the MHV-A59 ns2 protein involving the search for organ-specific proteins or RNAs that react differentially to wild-type and mutant ns2 proteins.

Coronaviruses are positive-stranded RNA viruses with genomes ranging in size from 27 to 32 kb. They are generally associated with respiratory and enteric infections and have long been recognized as important pathogens of livestock and companion animals (48). One of the hallmarks of coronaviruses is the pattern of multiple subgenomic mRNAs that are produced in infected cells by an unusual mechanism involving discontinuous genome transcription during minus-strand RNA synthesis (44). The recent emergence of the *Severe acute respiratory syndrome coronavirus* (SARS-CoV) (4) and an increased awareness of the extent of human coronavirus-associated disease (57) have renewed interest in this group of viruses.

The size and complexity of the coronavirus genome and the ability of coronaviruses to adapt to a range of different host species are remarkable. In this respect, it has been suggested that the gradual acquisition of several RNA-processing enzymes by the ancestors of contemporary coronaviruses may have improved the fidelity of RNA replication and transcription to allow for genome expansion (15). This, in turn, would provide coronaviruses with the opportunity to extend their host range and adapt rapidly to changing environmental conditions. For example, genome expansion may have allowed for the acquisition of genes that are able to antagonize host cell defense mechanisms or genes that facilitate virus replication by modulating cellular functions.

Basically, the coronavirus genome encodes three classes of proteins (30). First, it encodes structural proteins of the virus. These are the spike (S), membrane (M), envelope (E), and nucleocapsid (N) proteins and, for some viruses of group 2a, an additional hemagglutinin-esterase (HE) protein. Second, it encodes proteins that have a critical role in viral RNA synthesis. The majority of these are nonstructural proteins (nsp's) that are referred to as replicative proteins or proteins of the replicase-transcriptase complex (44). They include proteins common to many RNA viruses, such as proteinases (PL1/2^{pro} in nsp3 and M^{pro} in nsp5), RNA-dependent RNA polymerase (RdRp in nsp12), and 5′-to-3′ helicase (HEL in nsp13), as well as others that are unique to some or all coronaviruses and related viruses belonging to the order *Nidovirales* (15). These include a 3′-to-5′ exonuclease (ExoN in nsp14) and a uridylate-specific endoribonuclease (EndoU in nsp15) (62). Third, the genome encodes proteins that are not essential for virus rep-

* Corresponding author. Mailing address for Stuart G. Siddell: Department of Cellular and Molecular Medicine, School of Medical and Veterinary Sciences, University of Bristol, University Walk, Bristol BS8 1TD, United Kingdom. Phone: 0044 117 33 12067. Fax: 0044 117 33 12091. E-mail: stuart.siddell@bristol.ac.uk. Mailing address for Susan R. Weiss: Department of Microbiology, University of Pennsylvania School of Medicine, 203A Johnson Pavilion, 36th Street and Hamilton Walk, Philadelphia, PA 19104-6076. Phone: (215) 898-8013. Fax: (215) 573 -4858. E-mail: weisssr@mail.med.upenn.edu.

† J.K.R.-C. and H.S. contributed equally to this work.

‡ S.R.W., A.E.G., and S.G.S. are co-senior authors of the paper.

▽ Published ahead of print on 28 January 2009.

lication in cell culture but appear to confer a selective advantage in vivo. These are referred to as niche-specific, group-specific, or accessory proteins (9, 32, 44).

Although useful, this view of coronavirus proteins is obviously oversimplified. For example, there are virion proteins, such as the nucleocapsid (N) protein, that are clearly involved in intracellular viral RNA synthesis (45) and the modulation of cellular responses (59). Conversely, there are replicase-transcriptase proteins, such as the nsp3 protein, that are found in purified virions of, for example, SARS-CoV (37). Also, in terms of function, there are proteins that are apparently associated with only a single enzymatic activity, for example, M^{pro} in nsp5, and there are complex, multifunctional proteins, such as nsp3, which may have domains involved with enzymatic and structural roles in the biogenesis of the replicase-transcriptase complex, protease domains such as $PL1/2^{pro}$ with the additional potential to modify cellular proteins by deubiquitination, domains such as the poly(ADP-ribose)-binding domain (also known as ADP ribose 1″-phosphatase, ADRP, or X domain) with as-yet-undefined roles in the virus life cycle, and "orphan" domains such as the SARS-CoV-unique domain and other similarly positioned domains that are exclusively conserved in genetically compact subsets of coronaviruses (1, 20, 24, 25, 37, 39) (A. E. Gorbalenya, unpublished data). As we learn more, and extend the techniques and assays used to study coronaviruses, the simple distinctions between structural, nonstructural, and niche-specific proteins and the concept of essential and nonessential functions may become even less clear.

One of the earliest proteins identified as a coronavirus niche-specific protein was the *Murine hepatitis virus* (MHV) ns2 protein. This protein is encoded in open reading frame 2a (ORF2a) of most, but not all, coronaviruses of group 2a and is expressed from the largest subgenomic mRNA. The ns2 protein has a molecular mass of about 30 kDa (261 residues for MHV strain A59 [MHV-A59]), and it is localized to the cytoplasm (63). The protein is expressed in infected cells with the same kinetics as the virus structural proteins, but it has a relatively short half-life (2). It has been reported that the *Bovine coronavirus* ns2 protein is phosphorylated (6). Comparative sequence analysis has placed the coronavirus ns2 proteins within a family in a large superfamily of 2H phosphoesterase proteins including cellular RNA ligases and cyclic nucleotide phosphoesterases (CPD) that are distinguished by a pair of conserved His-x-Thr/Ser motifs implicated in catalysis (31, 50).

The function of the coronavirus ns2 protein has been a matter of speculation for many years. It was previously shown by Schwarz et al. (46) that the ns2 protein of MHV-JHM was not essential for virus replication in transformed mouse (DBT) cells, and those authors predicted that the function of the ns2 gene may be manifested only in vivo. However, this mutant strain of MHV-JHM, which is a neurotropic coronavirus, was found to be fully virulent for mice following intracranial (i.c.) inoculation (J. Leibowitz, personal communication; S. Perlman, personal communication). Subsequently, de Haan et al. (9) used targeted recombination to produce an MHV-A59 recombinant in which the coding region between ORF1b and the S protein-coding ORF (i.e., the region encoding ns2 and the HE protein) was deleted. Again, those authors showed that there was no difference in the single-step growth kinetics of this recombinant virus in mouse LR7 cells compared to parental wild-type virus. However, this mutant virus was significantly attenuated when inoculated into mice i.c. Finally, Sperry et al. (53) showed more recently that a recombinant MHV-A59 mutant with a single-amino-acid substitution of Leu with Pro at ns2 residue 94 is moderately attenuated for replication in mice following i.c. inoculation.

The results described above clearly suggest that MHV-A59 ns2 is a virulence factor for replication in vivo. However, the design of these experiments does not allow definitive conclusions. For example, the MHV-Δ2aHE mutants described previously by de Haan et al. have both the ns2 and HE genes deleted. This large genomic deletion could have subtle effects on viral replication due to its sheer size and regardless of the functions of the deleted genes, and these effects could be magnified during in vivo infections. Also, in both in vivo studies, only i.c. inoculation was investigated as a route of infection, and the virulence of the relevant mutants was determined only by the survival of animals in a 50% lethal dose assay.

In this paper, we report a bioinformatic-based, reverse genetic approach to study in more detail the in vivo phenotypes of viruses that have single, site-specific mutations in codons encoding residues predicted to be critical for the putative ns2 CPD activity of MHV-A59. We also investigated the pathogenesis of mutant virus following infection by both intrahepatic (i.h.) and i.c. routes of inoculation and assayed for virus replication by the measurement of organ-specific titers and immunohistochemistry. The results reveal that mutations of codons encoding catalytic-site ns2 residues selectively attenuate MHV-A59 infection in liver but not in the brain, implying that the presumed CPD activity of ns2 is important for virus replication in at least one organ. This finding also suggests that the role played by ns2 in the virus life cycle could be elucidated by the analysis of virus-host cell interactions in specific tissues of the infected animal.

MATERIALS AND METHODS

Structural modeling. A structural model of the amino-terminal two-thirds of the MHV-A59 ns2 protein was generated by using the HHpred server (http://toolkit.tuebingen.mpg.de/hhpred). HHpred builds a profile hidden Markov model from a query sequence and compares it with a database of hidden Markov models representing domains with known structures (52). The closest template proposed was the central domain of the rat A-kinase-anchoring protein, AKAP 18 delta (13). This aligned template was then used to predict a structural model for the MHV-A59 ns2 protein using MODELLER, which implements comparative protein structure modeling by satisfaction of spatial restraints (42). The accuracy of this model was assessed using Verify3D (29). PyMol (0.99rc6) (http://pymol.sourceforge.net/) was used for molecular graphics.

Cells and viruses. Mouse 17 clone 1 fibroblast cells (17Cl-1) (54), HeLa-D980R cells (26), and primary fibroblast cultures (mouse embryonic fibroblasts) derived from *129/SvJ* mouse embryos (38) were cultured at 37°C in Dulbecco's modified Eagle's medium supplemented with 10% fetal bovine serum, penicillin (100 U/ml), and streptomycin (100 μg/ml). Mouse L2 fibroblast cells were cultured in the same medium with HEPES (10 mM). Monkey kidney (CV-1) cells and baby hamster kidney (BHK-21) cells were obtained from the European Collection of Cell Cultures and cultured in minimal essential medium supplemented with HEPES (25 mM), 5% fetal bovine serum, and antibiotics. Plaque assays were done using 17Cl-1 or L2 cells as described previously (18, 43). Vaccinia virus (WR strain) and vaccinia virus recombinants were propagated, titrated, and purified as described previously (55).

Recombinant viruses. Recombinant inf-MHV-A59 and the recombinant mutants inf-ns2 H46A, inf-ns2 S48A, inf-ns2-S120A, and inf-ns2-H126R were derived from vaccinia virus vMHV-inf-1, which contains a cloned, full-length MHV-A59 cDNA (GenBank accession number AY700211). Mutagenesis was done using a reverse genetics system described previously (5). Briefly, two rounds

of vaccinia virus-mediated homologous recombination were done using the *Escherichia coli* guanine-phosphoribosyltransferase (GPT) gene as a selection marker. First, the ns2 protein-coding region within the vMHV-inf-1 cDNA was replaced by the GPT gene using homologous recombination with plasmid pGPT-ns2. pGPT-ns2 encodes the GPT gene flanked on its left by MHV-A59 nucleotides (nt) 20606 to 21641 and on its right by MHV-A59 nt 22679 to 24009. Second, the GPT gene within the recombinant vaccinia virus vMHV-ns2GPT cDNA was replaced by one of four mutated ns2 protein-coding regions using homologous recombination with plasmids pns2-H46A (MHV-A59 nt 21907 to 21909; CAT→GCT), pns2-S48A (MHV-A59 nt 21913 to 21915; AGT→GCT), pns2-S120A (MHV-A59 nt 22129 to 22131; UCC→GCC), and pns2-H126R (MHV-A59 nt 22147 to 22149; CAC→CGC). These plasmids were produced by site-directed PCR-mutagenesis of plasmid pns2rec, which contains MHV-A59 cDNA sequences corresponding to nt 19438 to 24004, including the ns2 protein-coding region (ORF2a) between nt 21772 and 22557. The identities of plasmids and recombinant vaccinia viruses were confirmed by sequence analysis of the mutated regions. Further cloning details, plasmid maps, and sequences are available from the authors on request.

Recombinant coronaviruses inf-MHV-A59, inf-ns2-H46A, inf-ns2-S48A, inf-ns2-H126R, and inf-ns2-S120A were rescued from cloned cDNA using purified, EagI-cleaved vaccinia virus DNA as a template for the transcription of recombinant, full-length MHV genomic RNA, which was electroporated in to BHK-MHV-N cells as described previously (5). Following electroporation, the transfected BHK-MHV-N cells were mixed with a fourfold excess of 17Cl-1 cells and cultured at 37°C. At days 1 and 2 postelectroporation, tissue culture supernatants were taken, and recombinant coronaviruses were plaque purified three times. Virus stocks were obtained by using virus from a single plaque to infect 17Cl-1 cells to yield passage 1 virus stocks with a titer greater than 1×10^8 PFU/ml. The identities of recombinant MHV-A59 and recombinant mutant viruses were confirmed by sequence analysis of the mutated regions.

Northern blotting. RNA for Northern blotting was obtained by infecting 17Cl-1 cells with virus at a multiplicity of infection (MOI) of 10, incubating the cells for 4 or 8 h at 37°C, and isolating total RNA using the Trizol reagent (Invitrogen, Paisley, United Kingdom) as described by the manufacturer. The poly(A)-containing RNA was isolated using oligo$(dT)_{25}$ Dynabeads (Dynal, Oslo, Norway) as previously described (56) and incubated with formamide (50%) and formaldehyde (2.2 M) at 70°C for 10 min. For each sample, the poly(A)-containing RNA from 2×10^6 cells was electrophoresed in 1% agarose gel containing 20 mM MOPS (3-*N*-morpholino-propanesulfonic acid) and 600 mM formaldehyde. After electrophoresis, the gel was soaked in 0.05 N NaOH, neutralized, and equilibrated with 20× SSC (3 M NaCl, 0.3 M sodium citrate, 1 mM EDTA) before vacuum blotting onto a nylon membrane (Optitran BA-S 83; Schleicher & Schuell, Sigma-Aldrich, Poole, United Kingdom). The RNA was cross-linked to the membrane using UV light, and MHV RNAs were detected by hybridization with a 466-bp, α-^{32}P random prime-labeled PCR product corresponding to sequences in the nucleocapsid protein ORF of the MHV-A59 genome (49).

Viral replication in the brain and liver. Three- to four-week-old male virus-free C57BL/6 mice purchased from the National Cancer Institute (Frederick, MD) were anesthetized with isoflurane (IsoFlo; Abbott Laboratories) for i.h. or i.c. inoculations. Virus was diluted in phosphate-buffered saline containing 0.75% bovine serum albumin. For i.h. infections, mice were inoculated with 500 PFU of inf-MHV-A59, inf-ns2-H46A, inf-ns2-S48A, inf-ns2-H126R, or inf-ns2-S120A in a total volume of 50 μl, and for i.c. infections, mice were inoculated with 50 PFU of inf-MHV-A59, inf-ns2-H46A, inf-ns2-S48A, inf-ns2-H126R, or inf-ns2-S120A in a total volume of 20 μl in the left cerebral hemisphere. At days 3, 5, and 7 postinoculation (p.i.), animals were sacrificed, livers were harvested from animals infected i.h., and brains and livers were harvested from animals infected i.c. Organs were placed in isotonic saline containing 0.167% gelatin (gel saline) and homogenized. Viral titers were determined by plaque assay on L2 fibroblasts (14). All mouse experiments were reviewed and approved by the University of Pennsylvania IACUC.

Immunohistochemistry. A small piece of the top left lobe of the liver and the right half of sagittally sectioned brain from animals sacrificed at day 5 p.i. were fixed in formalin, embedded in paraffin, sectioned, and stained for viral antigen. Antigen staining was done by the avidin-biotin-immunoperoxidase technique (Vector Laboratories) by using diaminobenzidine tetrahydrochloride as the substrate and a 1:20 dilution of a monoclonal antibody raised against MHV nucleocapsid (N) (kindly provided by Julian Leibowitz). Slides were counterstained with hematoxylin.

RESULTS

Rationale for design of mutants that target the active-site residues of the MHV-A59 ns2 protein. To study the role of ns2 in MHV infection, we decided to characterize mutants carrying substitutions in the active site of the putative enzyme. The MHV ns2 protein belongs to the 2H phosphoesterase protein superfamily, whose sequence signature includes a pair of conserved His-x-Thr/Ser motifs (Fig. 1). On the basis of the sequence alignments shown in Fig. 1A, we decided to produce four MHV-A59 mutant viruses: mutant inf-ns2-H46A (MHV-A59 nt 21907 to 21909; CAT→GCT), mutant inf-ns2-S48A (MHV-A59 nt 21913 to 21915; AGT→GCT), mutant inf-ns2-S120A (MHV-A59 nt 22129 to 22131; UCC→GCC), and mutant inf-ns2-H126R (MHV-A59 nt 22147 to 22149; CAC→CGC). The mutants inf-ns2-H46A and inf-ns2-H126R target the His residues of the conserved His-x-Thr/Ser motifs, which were substituted by either Ala (residue 46) or Arg (residue 126). The replaced residues were predicted to be part of the catalytic network of 2H phosphoesterase proteins (31, 50), implying that their replacement should be evident in test systems that rely upon CPD activity. The mutant inf-ns2-S48A targets a Ser residue of the first His-x-Thr/Ser motif. This residue is not thought to have a catalytic role but may be a co-coordinating residue involved in, for example, substrate binding (33). In our view, the effect of this mutation would depend upon the sensitivity of a test system and could range from unapparent to a phenotype equivalent to that caused by the substitution of a catalytic-site His residue. The mutant inf-ns2-S120A targets a Ser residue that is not thought to have any role in the catalytic or substrate binding activity of 2H phosphoesterase proteins but is located adjacent to the second His-x-Thr/Ser motif. We predicted this mutation to be neutral and without an associated phenotype.

Our mutation strategy was designed using a multiple-sequence alignment that was produced a number of years ago, a time at which none of the proteins of the 2H superfamily had been structurally characterized. In the meantime, crystallographic structures have been reported for several of these proteins, including a central domain of rat A-kinase-anchoring protein 18 delta ($AKAP18^{CD}$) (13). This domain is identified as being the closest template when the PDB70 protein structure database is queried with the MHV-A59 ns2 sequence. Figure 1B shows an alignment of MHV-A59 ns2 protein residues 6 to 187 and AKAP18 protein residues 89 to 291. This alignment reveals an approximate colinearity of the two His-x-Thr/Ser motifs, CM1 and CM2, as well as five alpha-helical regions ($\propto$1 to $\propto$5) and five beta-sheet regions (β1 to β5) that have been determined in the $AKAP18^{CD}$ molecule and are predicted for the MHV-A59 ns2 secondary structure. This extended alignment supports the placement of the MHV-A59 ns2 protein within the eukaryotic-viral LigT-like family (family II) of 2H phosphoesterases (31). We then continued to model the ns2 protein using the AKAP18 template in order to assess the effect of our mutation strategy in the context of the predicted tertiary organization of the MHV-A59 ns2 protein. Figure 1C shows that the ns2 protein can be modeled to produce an incomplete barrel-like structure with a large water-filled cavity that is characteristic of the 2H phosphoesterase superfamily of proteins. This structure places the conserved His46

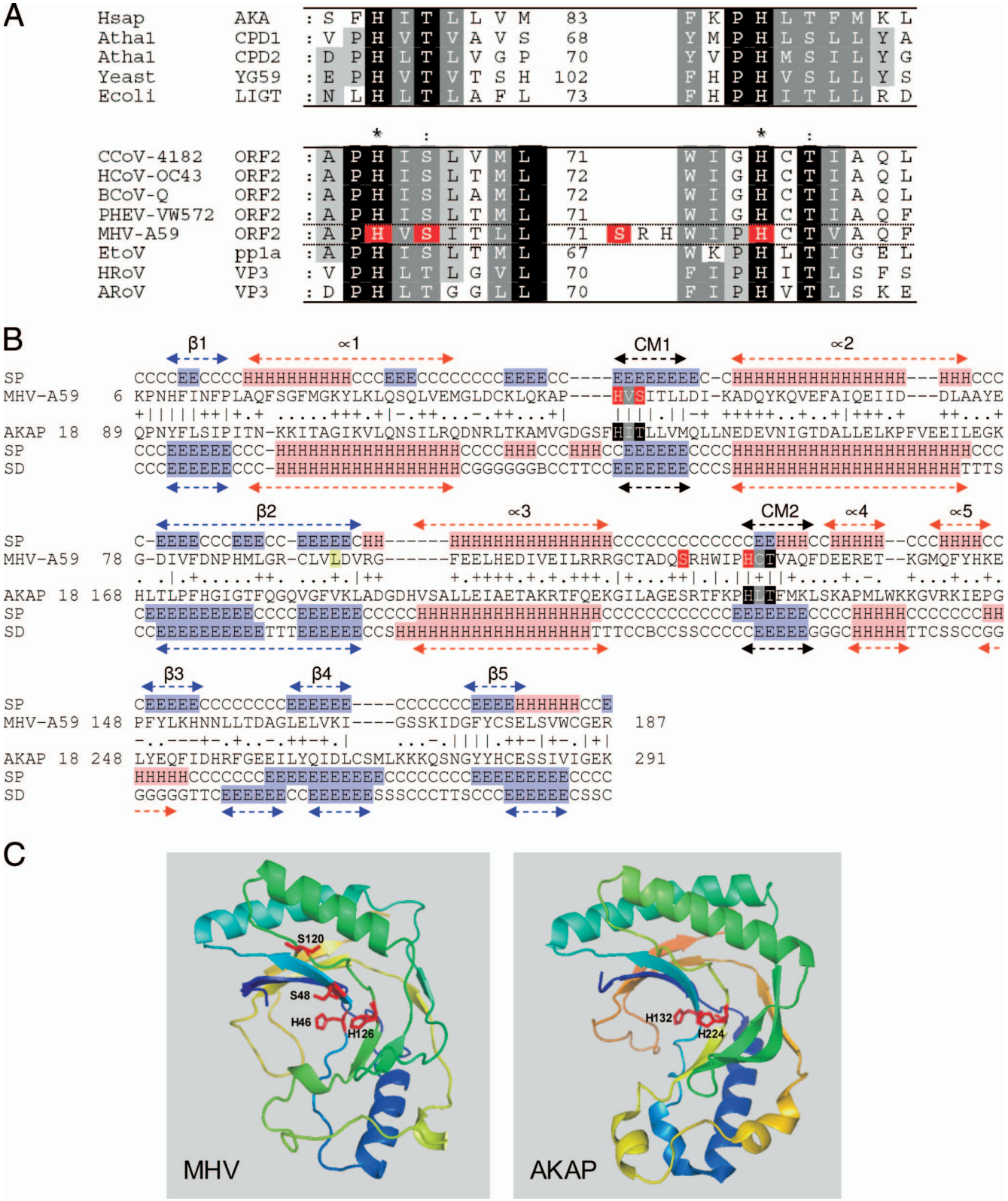

FIG. 1. Comparative structural analysis of the MHV-A59 ns2 protein. (A) Sequence-based alignment of the regions adjacent to the relevant His residues in cellular and viral proteins that belong to the CPD family of enzymes. The alignment is an extension of that reported previously (50). Residues are highlighted independently: black indicates absolutely conserved residues, and different shades of gray indicate different levels of conservation. Positions occupied by identical or similar residues in all proteins are indicated with an asterisks and colons. The MHV-A59 residues mutagenized in this study are highlighted with red. Hsap AKA, A-kinase-anchoring protein 18 gamma of *Homo sapiens* (GenBank accession number AAF28106) (this sequence is identical in the rat A-kinase-anchoring protein 18 delta); Athal CPD1, putative CPD1 of *Arabidopsis thaliana*

and His126 residues of the His-x-Thr/Ser motifs juxtaposed within the water-filled cavity. Ser48 is also facing into this cavity, while Ser120 lies in an adjacent loop region (31). The accuracy of this model can be assessed by comparison to a so-called three-dimensional profile (17), which is computed from the atomic coordinates of correct protein structures and is independent of whether the model has been derived by experimental or computational procedures (29). The model shown in Fig. 1C has a high profile score, especially in the region between residues 30 and 140, but is less reliable between residues 6 and 40 and in the region carboxyl terminal to residue 140 (Fig. 1B). Using the same criteria, in silico substitution of the relevant residues does not significantly decrease the quality of the model and suggests that the introduced changes, including the H126R substitution, would not have an impact upon the global structure of the MHV-A59 ns2 protein.

Viruses with mutations in the MHV-A59 ns2 gene replicate in mouse 17Cl-1 fibroblast cells and mouse embryonic cells. First of all, we tested the ability of recombinant MHV-A59 ns2 mutants to replicate in a transformed mouse cell line and primary embryonic cell cultures. Figure 2A shows that at an MOI of 10, the levels of replication of the parental inf-MHV-A59 and the recombinant MHV ns2 mutants inf-ns2-S48A, inf-ns2-H126R, and inf-ns2-S120A in 17Cl-1 cells were essentially indistinguishable. At both hour 6 postinfection and hour 12 postinfection, the supernatants from cultures infected with mutant viruses had reached titers that were equal to or greater than the titers of supernatants from cultures infected with the parental virus. Similarly, the replications of the parental inf-MHV-A59 and the recombinant MHV ns2 mutants inf-ns2-S48A, inf-ns2-H126R, and inf-ns2-S120A in primary embryonic mouse cells were also comparable, although at the same MOI of 10, the titers of virus reached in the embryonic cell cultures were 10- to 100-fold lower than those the 17Cl-1 cells (Fig. 2B). Immunofluorescence staining of the infected 17Cl-1 and primary embryonic cell cultures with MHV S-protein-specific monoclonal antibody 11F (41) showed that whereas more than 95% of the cells in the 17Cl-1 cultures had been infected, only about 5 to 10% of the cells in the primary cultures were infected (data not shown).

At the time that the experiments described above were done, the inf-ns2-H46A mutant was not available. However, subsequently, this mutant was analyzed and found to be indistinguishable from inf-MHV-A59 with respect to replication kinetics and plaque morphology in 17Cl-1 cell cultures (data not shown).

Viruses with mutations in the MHV-A59 ns2 gene synthesize viral RNA in infected 17Cl-1 cells. To confirm that the ns2 gene mutations in the recombinant viruses did not have a significant effect on virus replication in vitro, we analyzed viral RNA synthesis in 17Cl-1 cells infected with inf-MHV-A59 and the recombinant MHV-A59 ns2 mutants. Figure 3 shows that the mutant and wild-type viruses accumulated virus genomic and subgenomic poly(A)-containing RNA to equivalent levels at 8 h postinfection. The samples taken at 4 h postinfection suggest that the rates of RNA accumulation are also comparable, although it appears that wild-type inf-MHV-A59 may have synthesized slightly more virus RNA by this earlier time point. However, this result is not supported by the virus replication data shown in Fig. 2, and importantly, there is no obvious difference in the amounts of RNA synthesized in cells infected with the recombinant MHV-A59 ns2 mutants.

Viruses with mutations in the His46 and His126 codons of the MHV-A59 ns2 gene are attenuated in the liver. To assess the in vivo phenotype of the recombinant MHV-A59 ns2 mutants, C57BL/6 mice were inoculated i.h. with inf-MHV-A59, inf-ns2-H46A, inf-ns2-S48A, inf-ns2-H126R, or inf-ns2-S120A. Viral replication in the livers of infected animals was quantified by plaque assay of liver lysates from mice sacrificed at days 3, 5, and 7 p.i. (Fig. 4A). While the replication of inf-ns2-S48A and inf-ns2-S120A reached levels equivalent to those of inf-MHV-A59 at day 3 p.i., the replication of both inf-ns2-H46A and inf-ns2-H126R was significantly reduced ($P < 0.035$). This difference is even more evident at day 5 p.i., when inf-MHV-A59, inf-ns2-S48A, and inf-ns2-S120A reached peak titers in the liver, while the replication of inf-ns2-H46A and inf-ns2-H126R was significantly attenuated ($P < 0.0017$). All of the viruses were cleared from the liver by day 7 p.i.

To assess to abilities of these viruses to spread in the liver, the presence of MHV antigen was measured by immunohistochemical analysis of liver sections from mice sacrificed at day 5 p.i. (Fig. 4B), which corresponds to the peak of viral replication. Infection with inf-MHV-A59, inf-ns2-S48A, and inf-ns2-S120A resulted in focal areas of hepatocellular necrosis that colocalized with MHV antigen staining, consistent with the ability of these viruses to replicate to high titers in the liver. However, livers from animals infected with inf-ns2-H46A and inf-ns2-H126R had no obvious signs of antigen staining, con-

(accession number CAA16750); Athal CPD2, putative CPD2 of *Arabidopsis thaliana* (accession number CAA16751); yeast YG59, hypothetical 26.7-kDa protein of yeast (accession number P53314); Ecoli LIGT, 2′-5′ RNA ligase of *Escherichia coli* (accession number P37025); ns2, nonstructural protein (ORF2 encoded) of the coronaviruses CCoV-4182 (accession number ABG78746), HCoV-O43 (accession number AAA74377), bovine coronavirus strain Quebec (accession number P18517), PHEV-VW572, and MHV-A59 (accession number P19738); equine torovirus pp1a, C-terminal fragment of equine torovirus pp1a (accession number S11237); HRoV VP3, VP3 of human rotavirus (accession number BAA84964); ARoV VP3, VP3 of avian rotavirus PO-13 (accession number BAA24128). (B) Alignment of MHV-A59 ns2 protein residues 6 to 187 and AKAP18 protein residues 89 to 291. SP denotes the PSI-PRED secondary-structure prediction (21), and SD is the secondary structure assigned to the AKAP18 protein by DSSP (23). The symbols indicate the quality of the column-column match: [2], very good; +, good; •, neutral; −, bad. Predicted or determined regions of alpha-helix (H), beta-sheet (E), and random-coil (C) structures are indicated and numbered. The His-x-Thr/Ser motifs CM1 and CM2 are indicated, and critical residues are highlighted with dark gray or gray. The MHV-A59 residues mutagenized in this study, His46, Ser48, Ser120, and His126, are highlighted with red. The P94L mutation previously reported by Sperry et al. (53) is highlighted with yellow. (C) Ribbon representation of the predicted model of the MHV-A59 ns2 protein, amino acids 6 to 187, which was generated on the basis of the structure of the rat AKAP 18 delta protein, amino acids 89 to 291 (PDB accession number 2VFY). Both structures have been colored to highlight common regions of secondary structure. The His132 and His224 residues of AKAP 18 and the His46, Ser48, Ser120, and His126 residues of MHV-A59 ns2, which were substituted in this study, are shown as sticks in red.

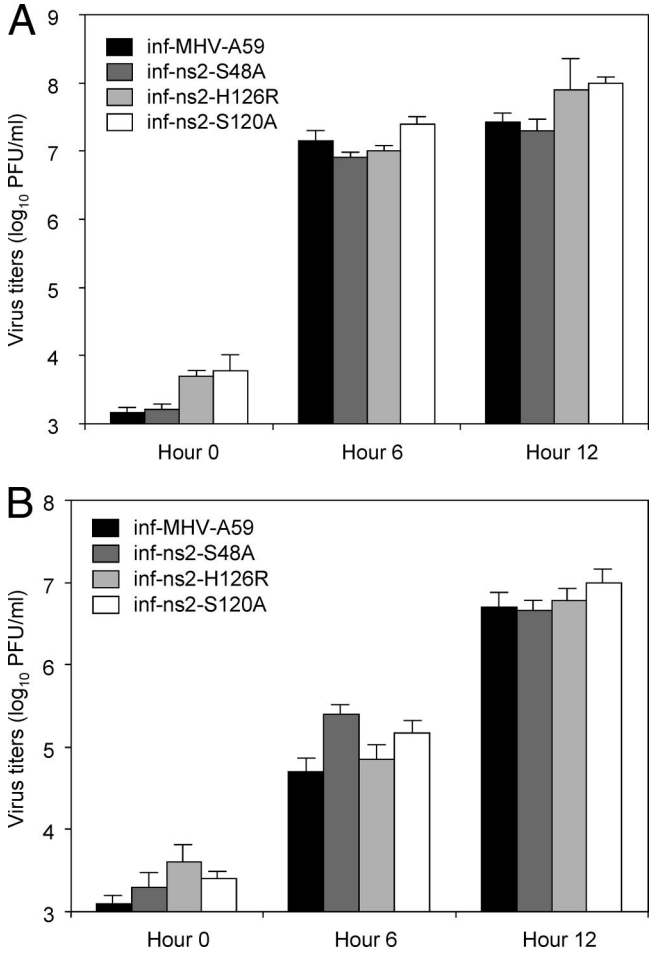

FIG. 2. Replication of recombinant inf-MHV-A59 and MHV-A59 ns2 mutants in mouse 17Cl-1 cells and mouse embryonic cells. Cultures of 17Cl-1 cells and mouse embryonic cells were infected with inf-MHV-A59, inf-ns2-S48A, inf-ns2-H126R, and inf-ns2-S120A at an MOI of 10 and incubated at 37°C. At hour 0, hour 6, and hour 12, samples of the culture supernatant were taken, and the titer of virus was measured. The error bars represent the standard deviations of means of data from triplicate plaque assays. There were no differences in the sizes or appearances of the plaques formed by inf-MHV-A59 and MHV-A59 ns2 mutants (data not shown).

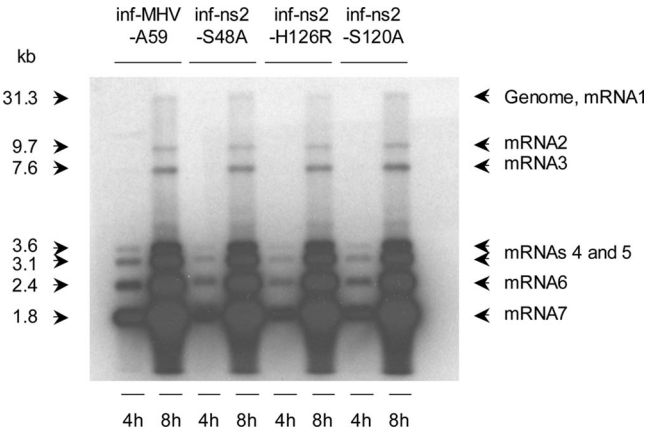

FIG. 3. Virus RNA synthesis in mouse 17Cl-1 fibroblast cells infected with recombinant MHV-A59 ns2 mutants. Cultures of 17Cl-1 cells were infected inf-MHV-A59, inf-ns2-S48A, inf-ns2-H126R, and inf-ns2-S120A at an MOI of 10 and incubated at 37°C. At hour 4 and hour 8, poly(A)-containing RNA was isolated from the infected cells and analyzed by Northern blotting. The sizes of MHV-A59 genomic and subgenomic RNAs are indicated in kilobases.

sistent with minimal levels of viral replication. In fact, the hepatic parenchyma looked normal in the livers from animals infected with inf-ns2-H46A and inf-ns2-H126R. These data indicate that the substitution of either of the conserved His residues of the canonical His-x-Thr/Ser motifs of MHV-A59 ns2 results in a severe attenuation of virus replication in the liver. In contrast, the substitution of either of the MHV-A59 ns2 residues Ser48 and Ser120 with alanine does not affect viral replication in the liver.

Viruses with mutations in the His46 and His126 codons of the MHV-A59 ns2 gene are not attenuated for replication in the brain. To investigate the ability of the recombinant MHV-A59 ns2 mutant viruses to replicate in the brain, another target of MHV replication, C57BL/6 mice, were inoculated i.c. with inf-MHV-A59, inf-ns2-H46A, inf-ns2-S48A, inf-ns2-H126R, or inf-ns2-S120A. Virus replications in both the brain (Fig. 5A) and the liver (Fig. 5B) were quantified by plaque assay at days 3, 5, and 7 p.i. All of the viruses replicated to equivalent titers in the brains of infected animals at all times p.i. Brain sections from mice infected with inf-MHV-A59, inf-ns2-H46A, inf-ns2-S48A, inf-ns2-H126R, or inf-ns2-S120A and sacrificed at day 5 p.i. exhibited similar levels of viral antigen when stained with anti-nucleocapsid antibody (Fig. 5C) and showed similar extents of inflammation (data not shown). However, consistent with the results obtained from mice infected by the i.h. route, the levels of replication of inf-ns2-H46A and inf-ns2-H126R were reduced in the livers compared to levels of replication of inf-MHV-A59, inf-ns2-S48A, or inf-ns2-S120A (Fig. 5B). These data show that while the His residues of the MHV-A59 ns2 His-x-Thr/Ser motifs are critical for virulence in the liver, they are not essential for replication in the brain.

We also point out that since the i.c. inoculations were carried out at a relatively low input of virus (50 PFU/animal), it is not surprising that, as exemplified by inf-MHV-A59, the kinetics of replication are slower and that the final levels of virus in the liver are lower than the 500 PFU/animal used for i.h. inoculation (Fig. 4A). Also, it is clear from Fig. 5B that the levels of replication of inf-ns2-S48A and inf-ns2-S120A in the liver following i.c. infection are lower than that of inf-MHV-A59 although statistically significant only for inf-ns2-S120A. Further studies are in progress, but it is possible that there is a subtle defect in spread from the brain to the liver of these mutants.

DISCUSSION

The results of this study lead to three main conclusions. First, as suggested by previous studies, we have now shown that the ns2 protein of MHV-A59 has an important role in virus pathogenicity, although it is not essential for virus replication in cell culture (9, 46, 53). Therefore, the MHV-A59 ns2 protein is similar to, for example, the nsp2 proteins of MHV and SARS-CoV (16) or the NS1 protein of avian influenza viruses (61), all of which are dispensable for in vitro replication but are

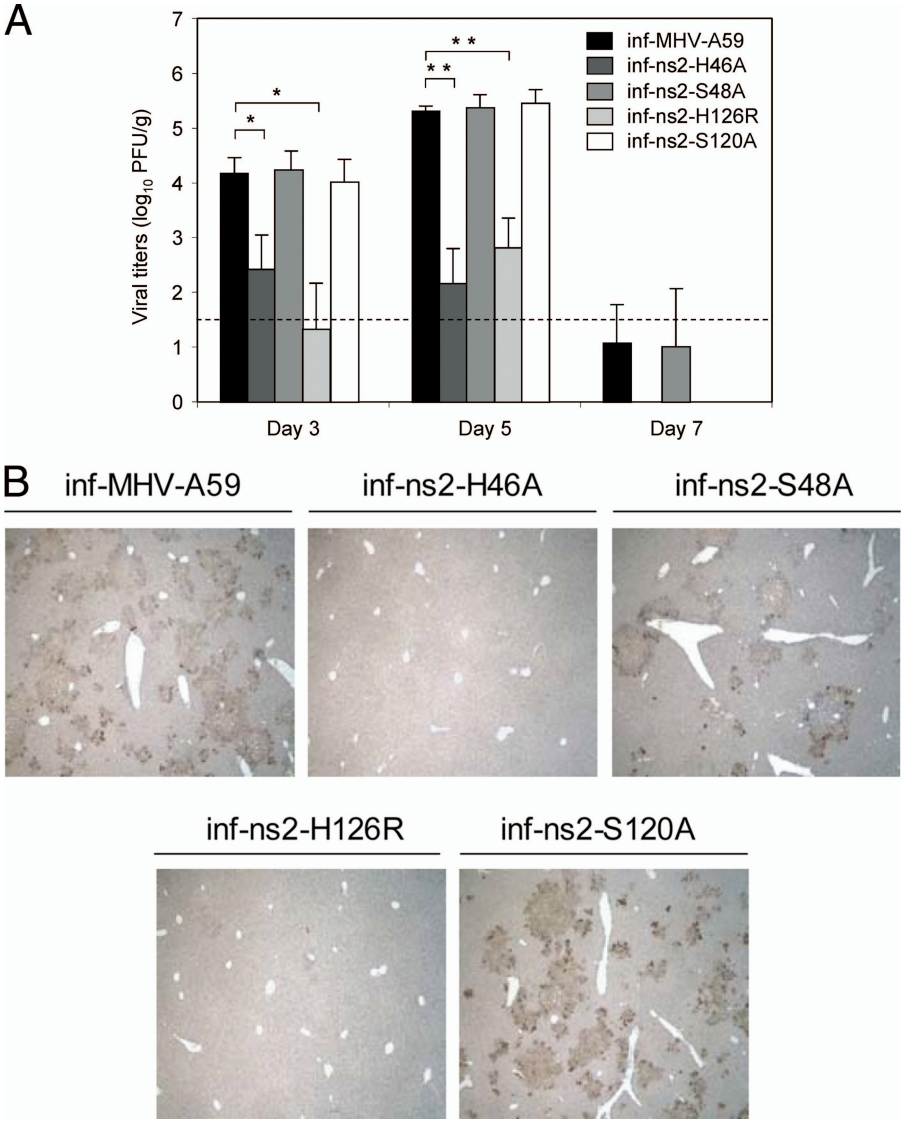

FIG. 4. Replication of wild-type and mutant viruses in the liver following i.h. inoculation. B6 mice were infected i.h. with 500 PFU of inf-MHV-A59, inf-ns2-H46A, inf-ns2-S48A, inf-ns2-H126R, or inf-ns2-S120A. (A) At days 3, 5, and 7 p.i., mice were sacrificed, and viral titers in the liver were determined by plaque assay on L2 cells. The dashed bar represents the limit of detection, and error bars represent standard errors of means ($n = 5$). Statistics were determined using a Student's t test. *, $P < 0.035$; **, $P < 0.0017$. (B) At day 5 p.i., livers were removed, fixed, and sectioned. MHV was detected with a monoclonal antibody against the nucleocapsid (N) protein using the avidin-biotin-immunoperoxidase technique. All data are derived from one representative experiment of two.

required for virulence in vivo. It is likely that many more coronavirus proteins will be added to this list as more-discerning animal models of coronavirus pathogenesis and virulence are developed (27, 60). Second, our results suggest that the function of the MHV-A59 ns2 protein is important for virus replication in the liver of infected animals but is not important for virus replication in the brain. Again, this phenotype has been recognized only because the murine models of MHV-A59 infection are well characterized and encompass both viral hepatitis and viral encephalitis as well as demyelinating, respiratory, and ocular disease (7, 47, 58). Third, our data provide further, albeit indirect, evidence that ns2 is enzymatically active. Specifically, the data that we have obtained are compatible with data from the original bioinformatics-based model predicting that the substitution of the probed residues would produce effects that correlate in magnitude with the conservation of the residues and their roles in other homologous proteins. In this study, the strongest attenuated phenotype was revealed only for mutants with a substitution of either of the two fully conserved and catalytic His residues, implying that the associated enzymatic activity, whatever it may be, is essential for MHV-A59 infection in liver.

The obvious question posed by our findings is the role of ns2 in the pathogenesis and virulence of MHV-A59 infection and the underlying molecular mechanism of ns2 action. As mentioned above, the MHV-A59 ns2 protein belongs to a large superfamily of proteins known as 2H phosphoesterases. Specifically, the MHV-A59 ns2 protein falls within the eukaryotic-

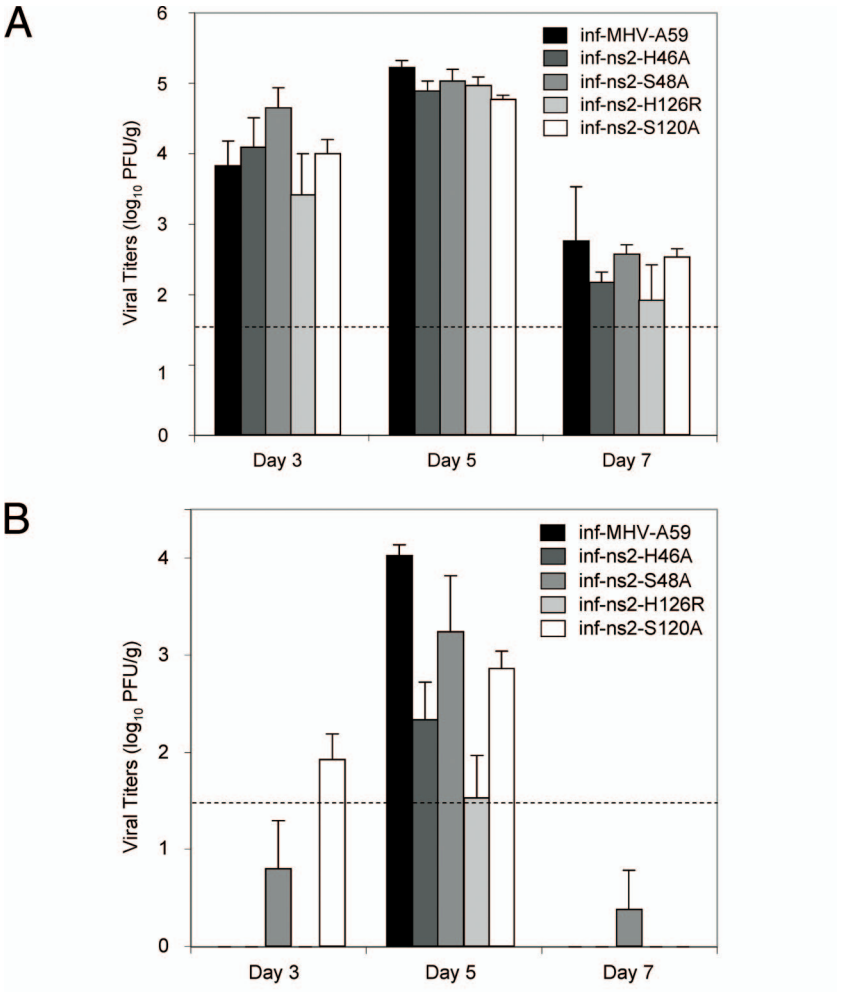
A
Viral Titers (log10 PFU/g)
6
5
4
3
2
1
0
Day 3
Day 5
Day 7
inf-MHV-A59
inf-ns2-H46A
inf-ns2-S48A
inf-ns2-H126R
inf-ns2-S120A
B
Viral Titers (log10 PFU/g)
4
3
2
1
0
Day 3
Day 5
Day 7
inf-MHV-A59
inf-ns2-H46A
inf-ns2-S48A
inf-ns2-H126R
inf-ns2-S120A
C
inf-MHV-A59
inf-ns2-H46A
inf-ns2-S48A
inf-ns2-H126R
inf-ns2-S120A

viral LigT-like family (family II) of 2H phosphoesterases, which is typified by the human CGI-18 protein (31). This protein is a component of the Asc-1 (activating signal cointegrator) transcription coactivator complex that facilitates the interaction of transcription factors with the basal transcription machinery (22). The LigT-like phosphoesterases include enzymes that are involved in nucleic acid metabolism, such as the 2′,3′-cyclic nucleotide phosphodiesterase activity associated with *Saccharomyces cerevisiae* tRNA ligase (trl1) during pre-tRNA splicing as well as enzymes that are involved in the metabolism of cyclic nucleotides and oligonucleotides, such as yeast CPD1p, which converts ADP-ribose-1″,2″-cyclic phosphate (Appr>p) to ADP-ribose-1″-phosphate (Appr-1″-p) (31). None of these activities have been demonstrated for the ns2 protein of coronaviruses or its distant torovirus homolog (10, 51).

While the MHV-A59 ns2 function remains to be elucidated, our results can be rationalized within the framework of several models. First, our data are compatible with data for a previously described model (50), which proposed the ns2 protein to be a 1″,2″-CPD that (in concert with ADRP activity residing in the X domain of nsp3) may drive the production of RNA molecules that undergo splicing or splicing-related processing events. In this context, there is the possibility that the synthesis of coronavirus RNAs may involve the endoribonuclease activity of nsp15, which would produce RNA molecules with 2′,3′-cyclic phosphate termini, similar to the 5′ exon fragment of tRNA splicing. The MHV ns2 protein could play a role in this hypothetical processing pathway, acting through either a 2′,3′-esterase activity, processing the 5′-end product of the nsp15-mediated endonuclease reaction, or a 1″,2″-esterase activity that converts Appr>p to Appr-1″-p. Interestingly, yeast CPD1p can process both types of cyclic phosphates (50). It is important that in any model implicating ns2 in the regulation of RNA processing (50), ns2 is expected to play only a modulatory role. This relatively minor role is in line with ns2 being encoded in a small subset of coronaviruses, but as such, the role could be sufficient to secure a niche-specific effect.

If MHV-A59 ns2 CPD activity does convert Appr>p to Appr-1″-p, it may not only influence upstream events but (possibly together with the putative ADRP activity of nsp3) also alter the patterns of mono(ADP-ribosyl)ation or poly(ADP-ribosyl)ation within the infected cell. It is interesting that recombinant MHV mutants with amino acid substitutions in the catalytic residues of the ADRP domain have also been shown to have an attenuated phenotype in vivo (12). It is clearly important to verify the predicted CPD activity of the MHV-A59 ns2 protein and identify its substrate and the molecular effects leading to the phenotypes of the mutant viruses described herein. Also, as with some other CPD-containing proteins, e.g., AKAP18 (13), the MHV-A59 ns2 protein may also have a nonenzymatic function. If ns2 is a multifunctional protein, its enzymatic and nonenzymatic activities may not be mutually exclusive.

We also report (S. R. Weiss and V. Thiel, unpublished data) that we have not found any evidence to suggest that the MHV ns2 protein is able to interfere with the production or signaling of type I interferon following virus infection. The inf-ns2-H126R mutant, like inf-MHV-A59, is unable to induce beta interferon, nor is its replication inhibited by beta interferon pretreatment, in L2 murine fibroblasts. Also, inf-MHV-A59 and the inf-ns2-H126R mutant induce beta interferon to similar extents following infection of bone marrow-derived macrophages, one of two cell types shown thus far to produce type I interferon in response to MHV infection (3, 40). Further studies will be carried out to determine if the MHV-A59 ns2 mutants are more sensitive to interferon in the relevant primary cell types.

The second major conclusion of our studies is that the function of the MHV-A59 ns2 protein is important for virus replication in the liver of infected animals but is not important for virus replication in the brain, although our studies cannot rule out more subtle defects in the pathogenesis of MHV-A59 ns2 mutants in the central nervous system. Also, it is interesting that nonhepatotropic MHV strain JHM (MHV-JHM) expresses an ns2 protein highly homologous to that of MHV-A59, encoding the same putative catalytic residues (46, 63). This implies that the ns2 protein alone is not sufficient to confer the ability to induce hepatitis. Consistent with this, we previously observed that a chimeric virus in which ORFs 1a, 1b, and 2 (including the ns2 gene) are derived from MHV-JHM and in which the rest of the genome is derived from MHV-A59 has a pathogenic pattern very similar to that of MHV-A59; that is, it causes hepatitis. The reciprocal chimera, in which ORFs 1a, 1b, and 2 are derived from MHV-A59 and the rest of the genome is derived from MHV-JHM, is nonhepatotropic (36). Thus, in the context of MHV-A59/MHV-JHM chimeric viruses, MHV-A59 ns2 is neither necessary nor sufficient for the induction of hepatitis.

This liver-specific attenuation phenotype described for inf-ns2-H46A and inf-ns2-H126R is reminiscent of that reported previously for a range of MHV mutants (8, 28, 34, 35) and indicates that replication in the liver may be a particularly sensitive in vivo assay of virus fitness. Although this conclusion does not, in itself, provide us with any further insight into the role of ns2 in the pathogenesis and virulence of MHV-A59 infection, it is important. For example, it shows how a niche-specific protein, which has probably been acquired from an outside source in a relatively recent ancestor of a genetically compact and small subset of coronaviruses, can be adapted to

FIG. 5. Replication of wild-type and mutant viruses in the brain and liver following i.c. inoculation. B6 mice were infected i.c. with 50 PFU of inf-MHV-A59, inf-ns2-H46A, inf-ns2-S48A, inf-ns2-H126R, or inf-ns2-S120A. At days 3, 5, and 7 p.i., mice were sacrificed, and viral titers in the brain (A) and liver (B) were determined by plaque assay on L2 cells. The dashed bar represents the limit of detection, and error bars represent standard errors of the means ($n = 5$). All data are derived from one representative experiment of two. (C) B6 mice were infected i.c. with 50 PFU of inf-MHV-A59, inf-ns2-H46A, inf-ns2-S48A, inf-ns2-H126R, or inf-ns2-S120A. The mice were sacrificed at days 5 and 7 p.i., and the brains were removed, fixed, and sectioned. MHV antigen was detected with a monoclonal antibody against the nucleocapsid (N) protein using the avidin-biotin-immunoperoxidase technique. Part of the midbrain, pons, medulla, and cerebellum are shown. The pattern of antigen staining in this region of the brain is similar to that observed previously for MHV-A59-infected animals (19).

profoundly alter the cell tropism and/or pathogenicity of MHV-A59. We acknowledge that further studies are needed to decipher whether or not the liver is the only organ where ns2 enzymatic activity is essential for MHV-A59 infection, and more studies are needed to assess the role and importance of ns2 as a virulence determinant among other coronaviruses that encode this protein. However, in our view, the ns2 protein is a remarkable illustration of virus evolution resulting from the interplay between the processes of RNA recombination and genome expansion. In this respect, it is also, perhaps, relevant to note that the expression of the MHV-A59 ns2 protein, like many but not necessarily all coronavirus niche-specific proteins, is mediated via a subgenomic mRNA. This observation implies that a niche-specific expansion in coronaviruses may require only a minor adjustment in the (preexisting) mechanisms that regulate gene expression. In other words, the unique gene repertoire, including enzymes such as the 3′-to-5′ exonuclease (ExoN in nsp14) that may be involved in controlling the fidelity of coronavirus RNA replication (11), combined with the versatility of expression afforded by the use of translationally independent subgenomic mRNAs, may empower coronaviruses to acquire and accommodate genes that readily expand their ecological niche.

Finally, the data presented here also suggest a strategy to investigate the function of the MHV-A59 ns2 protein. We propose that the search for organ-specific proteins that interact with wild-type and substituted ns2 proteins, together with comparative transcriptomic profiling of mouse liver, mouse brain, and mouse immune cells infected with inf-MHV-A59, inf-ns2-H46A, or inf-ns2-H126R, in vivo and in cell culture, will be one route to elucidating how the ns2 protein contributes to the pathogenesis of MHV-A59 in vivo. These experiments are in progress.

ACKNOWLEDGMENTS

This work was partially supported by Wellcome Trust grant 065487 to S.G.S., NIH grant NS-54695 to S.R.W., The Netherlands Bioinformatics Centre grant SP 3.2.2 to A.E.G., and a grant from the Swiss National Science Foundation to V.T. J.K.R.-C. was partially supported by NIH training grant NS-07180.

We thank Nicholas Gonatas for help with neuropathology, and A.E.G. thanks Olga Slobodskaya for discussions and Eric Snijder and Jessika Zevenhoven-Dobbe for collaboration on the functional characterization of the ns2 protein.

REFERENCES

1. **Barretto, N., D. Jukneliene, K. Ratia, Z. Chen, A. D. Mesecar, and S. C. Baker.** 2005. The papain-like protease of severe acute respiratory syndrome coronavirus has deubiquitinating activity. J. Virol. **79:**15189–15198.
2. **Bredenbeek, P. J., A. F. Noten, M. C. Horzinek, and W. J. Spaan.** 1990. Identification and stability of a 30-kDa nonstructural protein encoded by mRNA 2 of mouse hepatitis virus in infected cells. Virology **175:**303–306.
3. **Cervantes-Barragan, L., R. Zust, F. Weber, M. Spiegel, K. S. Lang, S. Akira, V. Thiel, and B. Ludewig.** 2007. Control of coronavirus infection through plasmacytoid dendritic-cell-derived type I interferon. Blood **109:**1131–1137.
4. **Cheng, V. C., S. K. Lau, P. C. Woo, and K. Y. Yuen.** 2007. Severe acute respiratory syndrome coronavirus as an agent of emerging and reemerging infection. Clin. Microbiol. Rev. **20:**660–694.
5. **Coley, S. E., E. Lavi, S. G. Sawicki, L. Fu, B. Schelle, N. Karl, S. G. Siddell, and V. Thiel.** 2005. Recombinant mouse hepatitis virus strain A59 from cloned, full-length cDNA replicates to high titers in vitro and is fully pathogenic in vivo. J. Virol. **79:**3097–3106.
6. **Cox, G. J., M. D. Parker, and L. A. Babiuk.** 1991. Bovine coronavirus nonstructural protein ns2 is a phosphoprotein. Virology **185:**509–512.
7. **De Albuquerque, N., E. Baig, X. Ma, J. Zhang, W. He, A. Rowe, M. Habal, M. Liu, I. Shalev, G. P. Downey, R. Gorczynski, J. Butany, J. Leibowitz, S. R. Weiss, I. D. McGilvray, M. J. Phillips, E. N. Fish, and G. A. Levy.** 2006. Murine hepatitis virus strain 1 produces a clinically relevant model of severe acute respiratory syndrome in A/J. mice. J. Virol. **80:**10382–10394.
8. **de Haan, C. A., M. de Wit, L. Kuo, C. Montalto-Morrison, B. L. Haagmans, S. R. Weiss, P. S. Masters, and P. J. Rottier.** 2003. The glycosylation status of the murine hepatitis coronavirus M protein affects the interferogenic capacity of the virus in vitro and its ability to replicate in the liver but not the brain. Virology **312:**395–406.
9. **de Haan, C. A., P. S. Masters, X. Shen, S. Weiss, and P. J. Rottier.** 2002. The group-specific murine coronavirus genes are not essential, but their deletion, by reverse genetics, is attenuating in the natural host. Virology **296:**177–189.
10. **Draker, R., R. L. Roper, M. Petric, and R. Tellier.** 2006. The complete sequence of the bovine torovirus genome. Virus Res. **115:**56–68.
11. **Eckerle, L. D., X. Lu, S. M. Sperry, L. Choi, and M. R. Denison.** 2007. High fidelity of murine hepatitis virus replication is decreased in nsp14 exoribonuclease mutants. J. Virol. **81:**12135–12144.
12. **Eriksson, K. K., L. Cervantes-Barragán, B. Ludewig, and V. Thiel.** 15 October 2008. Mouse hepatitis virus liver pathology is dependent on ADP-ribose 1″-phosphatase, a viral function conserved in the alpha-like supergroup. J. Virol. doi:10.1128/JVI.02082-08.
13. **Gold, M. G., F. D. Smith, J. D. Scott, and D. Barford.** 2008. AKAP18 contains a phosphoesterase domain that binds AMP. J. Mol. Biol. **375:**1329–1343.
14. **Gombold, J. L., S. T. Hingley, and S. R. Weiss.** 1993. Fusion-defective mutants of mouse hepatitis virus A59 contain a mutation in the spike protein cleavage signal. J. Virol. **67:**4504–4512.
15. **Gorbalenya, A. E., L. Enjuanes, J. Ziebuhr, and E. J. Snijder.** 2006. Nidovirales: evolving the largest RNA virus genome. Virus Res. **117:**17–37.
16. **Graham, R. L., A. C. Sims, S. M. Brockway, R. S. Baric, and M. R. Denison.** 2005. The nsp2 replicase proteins of murine hepatitis virus and severe acute respiratory syndrome coronavirus are dispensable for viral replication. J. Virol. **79:**13399–13411.
17. **Hendlich, M., P. Lackner, S. Weitckus, H. Floeckner, R. Froschauer, K. Gottsbacher, G. Casari, and M. J. Sippl.** 1990. Identification of native protein folds amongst a large number of incorrect models. The calculation of low energy conformations from potentials of mean force. J. Mol. Biol. **216:**167–180.
18. **Hingley, S. T., J. L. Gombold, E. Lavi, and S. R. Weiss.** 1994. MHV-A59 fusion mutants are attenuated and display altered hepatotropism. Virology **200:**1–10.
19. **Iacono, K. T., L. Kazi, and S. R. Weiss.** 2006. Both spike and background genes contribute to murine coronavirus neurovirulence. J. Virol. **80:**6834–6843.
20. **Imbert, I., E. J. Snijder, M. Dimitrova, J. C. Guillemot, P. Lecine, and B. Canard.** 2008. The SARS-coronavirus PLnc domain of nsp3 as a replication/transcription scaffolding protein. Virus Res. **133:**136–148.
21. **Jones, D. T.** 1999. Protein secondary structure prediction based on position-specific scoring matrices. J. Mol. Biol. **292:**195–202.
22. **Jung, D. J., H. S. Sung, Y. W. Goo, H. M. Lee, O. K. Park, S. Y. Jung, J. Lim, H. J. Kim, S. K. Lee, T. S. Kim, J. W. Lee, and Y. C. Lee.** 2002. Novel transcription coactivator complex containing activating signal cointegrator 1. Mol. Cell. Biol. **22:**5203–5211.
23. **Kabsch, W., and C. Sander.** 1983. Dictionary of protein secondary structure: pattern recognition of hydrogen-bonded and geometrical features. Biopolymers **22:**2577–2637.
24. **Kanjanahaluethai, A., Z. Chen, D. Jukneliene, and S. C. Baker.** 2007. Membrane topology of murine coronavirus replicase nonstructural protein 3. Virology **361:**391–401.
25. **Kanjanahaluethai, A., D. Jukneliene, and S. C. Baker.** 2003. Identification of the murine coronavirus MP1 cleavage site recognized by papain-like proteinase 2. J. Virol. **77:**7376–7382.
26. **Kerr, S. M., and G. L. Smith.** 1991. Vaccinia virus DNA ligase is nonessential for virus replication: recovery of plasmids from virus-infected cells. Virology **180:**625–632.
27. **Kopecky-Bromberg, S. A., L. Martinez-Sobrido, M. Frieman, R. A. Baric, and P. Palese.** 2007. Severe acute respiratory syndrome coronavirus open reading frame (ORF) 3b, ORF 6, and nucleocapsid proteins function as interferon antagonists. J. Virol. **81:**548–557.
28. **Leparc-Goffart, I., S. T. Hingley, M. M. Chua, X. Jiang, E. Lavi, and S. R. Weiss.** 1997. Altered pathogenesis of a mutant of the murine coronavirus MHV-A59 is associated with a Q159L amino acid substitution in the spike protein. Virology **239:**1–10.
29. **Luthy, R., J. U. Bowie, and D. Eisenberg.** 1992. Assessment of protein models with three-dimensional profiles. Nature **356:**83–85.
30. **Masters, P. S.** 2006. The molecular biology of coronaviruses. Adv. Virus Res. **66:**193–292.
31. **Mazumder, R., L. M. Iyer, S. Vasudevan, and L. Aravind.** 2002. Detection of novel members, structure-function analysis and evolutionary classification of the 2H phosphoesterase superfamily. Nucleic Acids Res. **30:**5229–5243.
32. **Narayanan, K., C. Huang, and S. Makino.** 2008. SARS coronavirus accessory proteins. Virus Res. **133:**113–121.
33. **Nasr, F., and W. Filipowicz.** 2000. Characterization of the Saccharomyces

cerevisiae cyclic nucleotide phosphodiesterase involved in the metabolism of ADP-ribose 1″,2″-cyclic phosphate. Nucleic Acids Res. **28:**1676–1683.
34. **Navas, S., S.-H. Seo, M. M. Chua, J. Das Sarma, E. Lavi, S. T. Hingley, and S. R. Weiss.** 2001. Murine coronavirus spike protein determines the ability of the virus to replicate in the liver and cause hepatitis. J. Virol. **75:**2452–2457.
35. **Navas, S., and S. R. Weiss.** 2003. Murine coronavirus-induced hepatitis: JHM genetic background eliminates A59 spike-determined hepatotropism. J. Virol. **77:**4972–4978.
36. **Navas-Martin, S., M. Brom, M. M. Chua, R. Watson, Z. Qiu, and S. R. Weiss.** 2007. Replicase genes of murine coronavirus strains A59 and JHM are interchangeable: differences in pathogenesis map to the 3′ one-third of the genome. J. Virol. **81:**1022–1026.
37. **Neuman, B. W., J. S. Joseph, K. S. Saikatendu, P. Serrano, A. Chatterjee, M. A. Johnson, L. Liao, J. P. Klaus, J. R. Yates III, K. Wuthrich, R. C. Stevens, M. J. Buchmeier, and P. Kuhn.** 2008. Proteomics analysis unravels the functional repertoire of coronavirus nonstructural protein 3. J. Virol. **82:**5279–5294.
38. **Prince, S. N., E. J. Foulstone, O. J. Zaccheo, C. Williams, and A. B. Hassan.** 2007. Functional evaluation of novel soluble insulin-like growth factor (IGF)-II-specific ligand traps based on modified domain 11 of the human IGF2 receptor. Mol. Cancer Ther. **6:**607–617.
39. **Putics, A., W. Filipowicz, J. Hall, A. E. Gorbalenya, and J. Ziebuhr.** 2005. ADP-ribose-1″-monophosphatase: a conserved coronavirus enzyme that is dispensable for viral replication in tissue culture. J. Virol. **79:**12721–12731.
40. **Roth-Cross, J. K., S. J. Bender, and S. R. Weiss.** 2008. Murine coronavirus mouse hepatitis virus is recognized by MDA5 and induces type I interferon in brain macrophages/microglia. J. Virol. **82:**9829–9838.
41. **Routledge, E., R. Stauber, M. Pfleiderer, and S. G. Siddell.** 1991. Analysis of murine coronavirus surface glycoprotein functions by using monoclonal antibodies. J. Virol. **65:**254–262.
42. **Sali, A., and T. L. Blundell.** 1993. Comparative protein modelling by satisfaction of spatial restraints. J. Mol. Biol. **234:**779–815.
43. **Sawicki, D., T. Wang, and S. Sawicki.** 2001. The RNA structures engaged in replication and transcription of the A59 strain of mouse hepatitis virus. J. Gen. Virol. **82:**385–396.
44. **Sawicki, S. G., D. L. Sawicki, and S. G. Siddell.** 2007. A contemporary view of coronavirus transcription. J. Virol. **81:**20–29.
45. **Schelle, B., N. Karl, B. Ludewig, S. G. Siddell, and V. Thiel.** 2005. Selective replication of coronavirus genomes that express nucleocapsid protein. J. Virol. **79:**6620–6630.
46. **Schwarz, B., E. Routledge, and S. G. Siddell.** 1990. Murine coronavirus nonstructural protein ns2 is not essential for virus replication in transformed cells. J. Virol. **64:**4784–4791.
47. **Shindler, K. S., L. C. Kenyon, M. Dutt, S. T. Hingley, and J. Das Sarma.** 2008. Experimental optic neuritis induced by a demyelinating strain of mouse hepatitis virus. J. Virol. **82:**8882–8886.
48. **Siddell, S. G., and E. J. Snijder.** 2008. An introduction to nidoviruses, p. 1–13. *In* S. Perlman, T. Gallagher, and E. J. Snijder (ed.), Nidoviruses. ASM Press, Washington, DC.
49. **Skinner, M. A., and S. G. Siddell.** 1983. Coronavirus JHM: nucleotide sequence of the mRNA that encodes nucleocapsid protein. Nucleic Acids Res. **11:**5045–5054.
50. **Snijder, E. J., P. J. Bredenbeek, J. C. Dobbe, V. Thiel, J. Ziebuhr, L. L. Poon, Y. Guan, M. Rozanov, W. J. Spaan, and A. E. Gorbalenya.** 2003. Unique and conserved features of genome and proteome of SARS-coronavirus, an early split-off from the coronavirus group 2 lineage. J. Mol. Biol. **331:**991–1004.
51. **Snijder, E. J., J. A. den Boon, M. C. Horzinek, and W. J. Spaan.** 1991. Comparison of the genome organization of toro- and coronaviruses: evidence for two nonhomologous RNA recombination events during Berne virus evolution. Virology **180:**448–452.
52. **Soding, J., A. Biegert, and A. N. Lupas.** 2005. The HHpred interactive server for protein homology detection and structure prediction. Nucleic Acids Res. **33:**W244–W248.
53. **Sperry, S. M., L. Kazi, R. L. Graham, R. S. Baric, S. R. Weiss, and M. R. Denison.** 2005. Single-amino-acid substitutions in open reading frame (ORF) 1b-nsp14 and ORF 2a proteins of the coronavirus mouse hepatitis virus are attenuating in mice. J. Virol. **79:**3391–3400.
54. **Sturman, L. S., and K. K. Takemoto.** 1972. Enhanced growth of a murine coronavirus in transformed mouse cells. Infect. Immun. **6:**501–507.
55. **Thiel, V., J. Herold, B. Schelle, and S. G. Siddell.** 2001. Infectious RNA transcribed in vitro from a cDNA copy of the human coronavirus genome cloned in vaccinia virus. J. Gen. Virol. **82:**1273–1281.
56. **Thiel, V., A. Rashtchian, J. Herold, D. M. Schuster, N. Guan, and S. G. Siddell.** 1997. Effective amplification of 20-kb DNA by reverse transcription PCR. Anal. Biochem. **252:**62–70.
57. **van der Hoek, L.** 2007. Human coronaviruses: what do they cause? Antivir. Ther. **12:**651–658.
58. **Weiss, S. R., and S. Navas-Martin.** 2005. Coronavirus pathogenesis and the emerging pathogen severe acute respiratory syndrome coronavirus. Microbiol. Mol. Biol. Rev. **69:**635–664.
59. **Ye, Y., K. Hauns, J. O. Langland, B. L. Jacobs, and B. G. Hogue.** 2007. Mouse hepatitis coronavirus A59 nucleocapsid protein is a type I interferon antagonist. J. Virol. **81:**2554–2563.
60. **Yount, B., R. S. Roberts, A. C. Sims, D. Deming, M. B. Frieman, J. Sparks, M. R. Denison, N. Davis, and R. S. Baric.** 2005. Severe acute respiratory syndrome coronavirus group-specific open reading frames encode nonessential functions for replication in cell cultures and mice. J. Virol. **79:**14909–14922.
61. **Zhu, Q., H. Yang, W. Chen, W. Cao, G. Zhong, P. Jiao, G. Deng, K. Yu, C. Yang, Z. Bu, Y. Kawaoka, and H. Chen.** 2008. A naturally occurring deletion in its NS gene contributes to the attenuation of an H5N1 swine influenza virus in chickens. J. Virol. **82:**220–228.
62. **Ziebuhr, J.** 2008. Coronavirus replicative proteins, p. 65–81. *In* S. Perlman, T. Gallagher, and E. J. Snijder (ed.), Nidoviruses. ASM Press, Washington, DC.
63. **Zoltick, P. W., J. L. Leibowitz, E. L. Oleszak, and S. R. Weiss.** 1990. Mouse hepatitis virus ORF 2a is expressed in the cytosol of infected mouse fibroblasts. Virology **174:**605–607.